Large-Scale Co-aggregation of Fluorescent Lipid Probes with Cell Surface Proteins

James L. Thomas,* David Holowka,‡ Barbara Baird,‡ and Watt W. Webb§

*Department of Physics, ‡Department of Chemistry, and §School of Applied and Engineering Physics, Cornell University, Ithaca, New York 14853

Abstract. Large scale aggregation of fluorescein-labeled immunoglobulin E (IgE) receptor complexes on the surface of RBL cells results in the co-aggregation of a large fraction of the lipophilic fluorescent probe 3,3'-dihexadecylindocarbocyanine (diI) that labels the plasma membranes much more uniformly in the absence of receptor aggregation. Most of the diI molecules that are localized in patches of aggregated receptors have lost their lateral mobility as determined by fluorescence photobleaching recovery. The diI outside of patches is mobile, and its mobility is similar to that in control cells without receptor aggregates. It is unlikely that the co-aggregation of diI with IgE receptors is due to specific interactions between these components, as two other lipophilic probes of different structures are also observed to redistribute with aggregated IgE receptors, and aggregation of two other cell surface antigens also results in the coredistribution of diI at the RBL cell surface. Quantitative analysis of CCD images of labeled cells reveals some differences in the spatial distributions of co-aggregated diI and IgE receptors. The results indicate that cross-linking of specific cell surface antigens causes a substantial change in the organization of the plasma membrane by redistributing pre-existing membrane domains or causing their formation.

SINCE the "fluid mosaic" model of cell membranes was presented by Singer and Nicholson in 1972 (27), much experimental evidence has accumulated to support the notion that the membrane is a fluid; i.e., that many molecules in the membrane are free to undergo lateral diffusion. Nonetheless, in many instances modifications to this model are necessary. For example, many cell types exhibit polarity, with different regions of the plasma membrane specialized for different functions. Epithelial cells (17), neuroblastoma cells (16), hepatocytes (18), osteoblasts (33), sperm (5), and egg (6) all show regional variations in membrane composition. In epithelia, these variations are thought to be maintained by tight junctions with adjacent cells in the confluent monolayer. In the other cell types, regional variation is maintained without tight junctions, through mechanisms that are not yet understood.

Just as some cells maintain large, functionally distinct regions of plasma membrane, they may also maintain smaller, perhaps submicroscopic domains with distinct physical and chemical properties. The concept of lipid microdomains was discussed as early as 1977, in the review article by Jain and White (14). They pointed out that evidence for microdomains of lipid was then available from freeze-fracture electron microscopy, differential scanning calorimetry, reflectivity measurements, and x-ray diffraction measurements. Scher and Bloch (26) have recently described the enhanced labeling of acetylcholine receptor-enriched regions of myotube plasma membranes with diI. Their results suggest that these receptors are located in specialized membrane domains that are controlled by other cellular proteins.

Other evidence for plasma membrane heterogeneity has been obtained from fluorescence photobleaching measurements of lipophilic probes. Wolf et al. have observed that only 36–77% of diI is free to diffuse laterally when incorporated into sea urchin egg plasma membrane (36), and only 65–82% is free to diffuse when incorporated into mouse egg plasma membrane (35). Dictus et al. (6) found that only 50% of the lipophilic probes 5-(N-hexadecanoyl)-aminofluorescein and 5-(N-tetradecanoyl)-aminofluorescein is free to diffuse laterally in *Xenopus* eggs. In neuronal membranes, Treistman et al. (32) found that the probes 1-acyl-2-(6-[N-(7-nitrobenz-2-oxa-1,3-diazo-4-yl)] aminohexanoyl) phosphatidylcholine (NBD-C_6-PC)[1] and rhodamine-phosphatidylethanolamine had diffusing fractions of roughly 60%, which decreased to 30% as the temperature was lowered from 25 to 4°C. Yechiel et al. (38) found that a headgroup-labeled NBD-phosphatidylethanolamine had a diffusing fraction less

Address all correspondence to Dr. Watt W. Webb, School of Applied and Engineering Physics, Cornell University, Ithaca, NY 14853.

1. *Abbreviations used in this paper*: BSS, buffered salt solution; diI, 3,3'-dihexadecylindocarbocyanine; FPR, fluorescence photobleaching recovery; NBD-C_6-PC, nitrobenzoxadiazole phosphatidylcholine; ORB, octadecyl rhodamine B; IgE, immunoglobulin E.

than 60% in young rat myocyte explants. More recently, experiments by Yechiel and Edidin (37) and Edidin and Stroynowski (7), in which the size of the bleaching spot was varied, showed monotonically decreasing diffusing fractions of NBD-C_6-PC and cell surface protein as the spot size was increased. In their experiments on human fibroblasts, the diffusing fraction of this lipid probe decreased from 90% at a spot diameter of 0.7 μm to 30% at a spot diameter of 5.0 μm. They argue that these results are indicative of micrometer-scale domains in the plasma membrane.

We report here observations of the membrane structure of RBL cells, as elucidated through the behavior of several lipophilic membrane probes. These probes generally distribute almost uniformly over the membrane, at optical resolution, in untreated RBL cells, and have nearly complete lateral mobility. When cell surface proteins (IgE receptor, 3D12 antigen) or a ganglioside (AA4 antigen) are aggregated by cross-linking with antibodies, a large fraction of the lipid probes colocalize with the aggregates and lose their lateral mobility, as determined by fluorescence photobleaching recovery measurements (FPR). These results suggest that certain lipids may preferentially segregate in specialized membrane domains in the plasma membrane that are either gathered together or induced to form upon aggregation of specific membrane components.

Materials and Methods

Labeling of Cells

RBL cells (subtype 2H3) were grown in stationary culture, and in some experiments their high affinity IgE receptors FcεRI, were bound to fluorescein isothiocyanate-labeled mouse IgE (FITC-IgE), as described previously (24). FITC-IgE preparations had 7 to 10 fluoresceins per IgE, determined by UV-vis absorption spectroscopy. After harvesting with EDTA, cells were centrifuged for 10 min at 1,000 rpm in a Beckman TS centrifuge, and then resuspended in a buffered salt solution: 135 mM NaCl, 5 mM KCl, 20 mM Hepes, 1 mM $MgCl_2$, 1.8 mM $CaCl_2$, 50 mM glucose, pH 7.4 (BSS) with 0.5 mg/ml BSA. The cells were typically divided into 0.5–1.0 ml aliquots at 3–5 × 10^6 cells per ml. The lipid probes dil or octadecyl rhodamine B (ORB) (both from Molecular Probes, Inc., Eugene, OR) were dissolved in methanol and added to cells at room temperature; the cells were mixed immediately and placed on ice for 10 min to allow incorporation of the probes into the plasma membrane. The standard concentrations of probes and solvents are as follows: for dil, either 10 μl of 0.2 mg/ml or 2 μl of 1.0 mg/ml in methanol was added to 500 μl of cells; for ORB, 5 μl of 0.2 mg/ml in methanol was added to 500 μl of cells. The labeled cells at 4°C were then diluted 5–10-fold in cold BSS, centrifuged and washed once in this buffer, and then resuspended at 3–5 × 10^6 cells/ml.

To cross-link IgE receptors, affinity purified polyclonal rabbit anti-mouse IgE (19) was added to the cells to a final concentration of 10 μg/ml. Cells were kept at 4°C for at least two hours to permit the formation of submicrometer-sized cell surface aggregates. To form larger aggregates of the IgE-receptor complex, cells were then warmed at 37° for 5–10 min, then cooled on ice. Control cells without anti-IgE were treated identically. For labeling of other surface antigens, either purified monoclonal antibody 3D12 (a gift of Dr. Henry Metzger) or AA4 (2) (10) (a gift of Dr. Reuben Siraganian) were incubated with dil-labeled cells at 10 μg/ml for 1 h at 4°C, and then the cells were washed once with cold BSS before incubation with 10 μg/ml of FITC-rabbit anti-mouse IgG (Cappel Research Products, Durham, NC) and treated as described for samples containing anti-IgE.

The amount of dil associated with the cells was estimated in two ways. First, the absorbance of dil at 562 nm in the supernatants after centrifugation of labeled cells ($A_{unbound}$) was measured and compared to that of dil added to buffer in the absence of cells (A_{total}). The maximum amount of cell-associated dil is then

$$[\text{diI}]_{cell} = \frac{A_{total} - A_{unbound}}{A_{total}} [\text{diI}]_{total}$$

For dil labeling at concentrations ranging from 0.2 μg/ml to 4 μg/ml, ~30% (0.03–0.7 nanomoles) of the dil added becomes associated with the cells as assessed by this method. With a cell surface area of ~1,000 μm^2 (21), and 20 $Å^2$/per alkyl chain in dil, the area fraction of the dye is roughly 0.4–8%. This represents an upper limit on the amount of dil incorporated into the plasma membrane, since some dye may be present as aggregates and a small amount may stain internal organelles. A direct estimate of the amount of dye incorporated into the plasma membrane has been made as follows: (*a*) the efficiency of the microscope was measured by using condenser illumination of known intensity (13 nW) and wavelength (530 nm), and noting the resultant CCD signal level (46 U). (*b*) The signal level from the cells (ca. 300 U in patched regions for the 4 μg/ml dil staining concentration) was compared to this signal from a known source. A correction for the optical acceptance solid angle was applied to the cell signal: for N.A. 1.25, 22% of the emitted fluorescent photons are captured by the microscope. The result is the total power radiated by the dye, ~19 nW. (*c*) The Hg lamp illumination intensity was measured as 12 mW. From the known absorption coefficient (133,000 L/mol-cm) and approximate quantum efficiency (0.5) of dil, the approximate number of fluors was found to be ~2.3 × 10^4 per μm^2, or an area fraction of ~1%, for cells stained with 4 μg/ml dil. This represents a lower limit on the amount of dye incorporated under these conditions, since some self quenching may occur.

In several experiments, the lipid probe was added to the cells after the formation of aggregates. Cells were warmed briefly (10 min) in a 37°C water bath, and then dil in methanol was added as above and the cells were placed on ice for 10 min, followed by centrifugation and resuspension at 4°C.

Microscopy

Cells in suspension were plated on coverslips for 10 min at 37°C, which permits cell adhesion and immobilization without significant changes in the spherical suspension morphology. The cells were then examined with a Zeiss universal microscope equipped for epi-fluorescence. An HBO 100W mercury arc lamp was used. Excitation filters were 488 nm narrow pass (10 nm) for FITC and 546 nm narrow pass (10 nm) for dil and ORB (Omega Optical, Brattleboro, VT); emission filters were 520 nm bandpass (20 nm) for FITC (Omega Optical) and OG580 (long pass) for dil and ORB (Schott Glass). The contribution of the fluorescein-labeled IgE to the dil signal was evaluated with cells labeled with only FITC-IgE. These cells had a fluorescence intensity of less than 1% of dil-labeled cells, when examined in dil optics. Similarly, cells labeled with only dil produced no significant fluorescence when illuminated with fluorescein optics. The positions of images of a graticule were noted with each emission filter set and used to correct for a slight lateral shift.

Images were taken with a Photometrics (Phoenix, AZ) CC200 CCD camera. Exposure times for images of dil were 0.2 s; for ORB, 0.8 s; and for FITC-IgE, 2.0 s. Cells were at room temperature (25°C) for all images. Images of lipid analog and IgE-receptor distributions were taken within 30 s of each other. There is no perceptible movement of patches over the course of at least several minutes at room temperature. Images were processed with a Recognition Concepts (Incline Village, NV) Trapix 55256 image processor accompanied by a Micro VAX II (Digital Equipment Corp.) computer.

FPR Measurements

Spot photobleaching measurements were made on cells at room temperature (25°C), as described elsewhere (4) (31). Photon counting and data acquisition were performed with a Stanford Research SR400 preamplifier and SR440 discriminator/photon counter, interfaced to the Micro VAX via GPIB (National Instruments). The fluorescence recovery curves were fit by non-linear least squares to

$$F(t) = \frac{F(0) + F(\infty)(t/t_{1/2})}{1 + (t/t_{1/2})}$$

where F(t) is the fluorescence at time t after bleaching, F(0) is the intensity immediately after bleaching, F(∞) is the asymptotic fluorescence level following recovery after photobleaching, and $t_{½}$ is the recovery half-time. The diffusion coefficient, D, is determined from $t_{½}$ and the spot size, with a correction for bleach depth as described in reference (39). The $1/e^2$ intensity spot diameter of the Gaussian beam was determined to be 2.0 ± 0.1 μm by measuring the size of a spot bleached in a thin formvar/dil film. Mobile fractions are defined by

$$\frac{F(\infty) - F(0)}{F_{PB} - F(0)}$$

where F_{PB} is the fluorescence intensity before bleaching. The position of best focus for photobleaching experiments was determined by first focusing visually on the cell surface not attached to the glass coverslip, and then maximizing the photocounts under monitor laser beam illumination. This procedure was necessary, since changing filters (to acquire both FITC and dil images) on the Zeiss Universal microscope always produced some small vibration and defocusing.

Results

Colocalization of dil and Patched FITC-IgE

In the absence of cross-linking ligands, both IgE-receptor complexes and the lipid probe dil appear to be unaggregated on the cell surface. Fig. 1 shows the distribution of uncross-linked FITC-IgE at the coverslip plane (*A*) and at the cell equator (*C*). Also shown are the distributions of dil at the coverslip plane (*B*) and at the cell equator (*D*) of the same RBL cell. Under these conditions, both FITC-IgE and dil show relatively uniform ring staining at the cell equator (Fig. 1, *C* and *D*), similar to results obtained previously for fluorescently labeled IgE-receptor complexes (19). For both dil and FITC-IgE, relatively small variations in fluorescence are seen at the coverslip plane (Fig. 1, *A* and *B*). These variations are likely to be due primarily to morphological irregularities, particularly inhomogeneous distributions of unresolved microvilli at the cell surface. Electron microscopy has indicated that these receptors are abundant on microvilli before cross-linking (13) (29). (It is possible that some dil is preferentially associated with IgE receptors before their aggregation, but this issue cannot be resolved by fluorescence microscopic analysis.)

At temperatures above 15°C, aggregation of IgE receptors by cross-linking with anti-IgE leads to internalization with half-times that range from >30 min at 25°C (24) to ~10 min at 37°C (19). However, if the IgE receptors are cross-linked at 4°C, internalization is prevented, and small patches of IgE-receptor complexes become clearly visible by fluorescence microscopy over the course of several hours. Once formed, these patches do not readily internalize (as judged by microscopy and steady-state fluorescence spectroscopy [20]) even when the temperature is raised to 37°C. Rather, when the temperature is raised the small patches coalesce to form a large aggregated, open network at the cell surface (Fig. 2, *A* and *C*). When cells have been labeled with the lipophilic probe dil before cross-linking, the probe clearly colocalizes to the IgE-receptor patches on virtually every cell. This is illustrated in Fig. 2 for a single cell, where photo A is the distribution of FITC-IgE with the microscope focused at the coverslip where the cell is flattened. Photo B is the distribution of dil at the same focal plane: the pattern of fluorescence coincides with the patched IgE receptor. Photo C is the same cell focused at the equator of the cell, showing the FITC-IgE fluorescence in discrete patches on the cell surface, seen at the circumference. (The hazy fluorescence "inside" the cell actually arises from the out-of-focus top and bottom surfaces.) Photo D shows the dil fluorescence at the same equatorial focus. Again, there is correspondence between the dil fluorescence distribution and the patches of IgE receptor. Typically, about half of the plasma membrane dil is aggregated into the patches (determined by integrating dil fluorescence intensity over areas on and off patches).

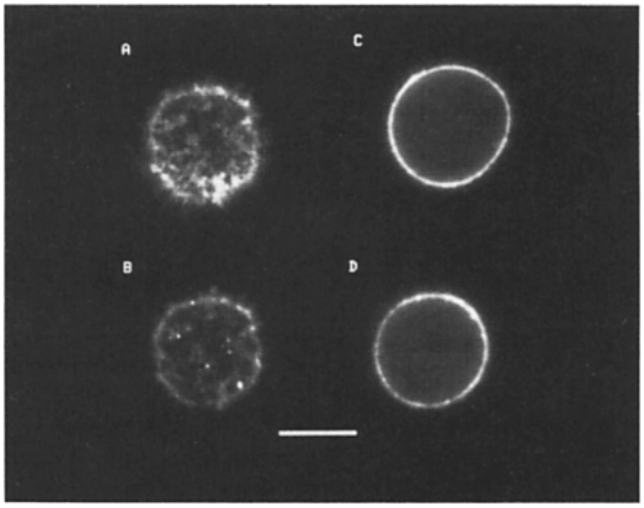

Figure 1. Uncross-linked cells exhibit fluorescence that is relatively uniform. *A* shows the FITC-IgE distribution at the coverslip; *B* shows the dil distribution for the same cell and same focal plane. *D* is the same cell, showing the dil distribution at the equator, while *C* is a typical equatorial FITC-IgE distribution (on a different cell from that in *A*, *B*, and *D*). Bar, 10 μm.

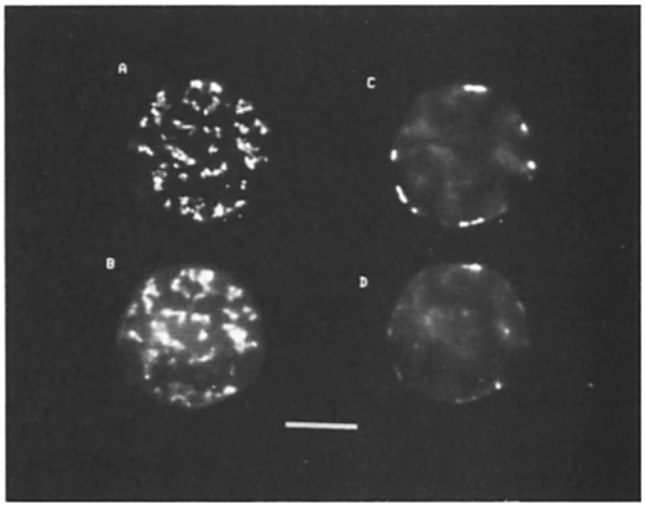

Figure 2. Colocalization of the lipophilic probe dil with patched IgE receptor. *A* and *C* are FITC-IgE images of a single RBL cell, focused at the coverslip and the cell equator, respectively. *B* and *D* are dil images of the same cell at the same focal planes as *A* and *C*, respectively. Bar, 10 μm.

The coincidence of dil fluorescence with FITC-IgE receptor aggregates is seen over at least a tenfold range of dil membrane concentrations (<0.8 to 8 area %), indicating that phase separation of the dil is not likely to play a role in the co-aggregation process. Furthermore, when dil is added after patches of IgE receptor are formed as described in Materials and Methods, coincidence of the dil fluorescence with the IgE receptor aggregates is also seen. When labeled with 4 μg/ml dil, the molar ratio of cell-associated dil to IgE receptors is estimated to be at least 50:1, determined either from the dil fluorescence intensity or from the amount of dye that spins down with the cells. Even at this membrane concentration, dil has no significant effect on the ability of the

cells to mobilize Ca^{+2} in response to IgE receptor aggregation (Holowka, D., unpublished results).

Quantitative analysis of the substrate-focused images 2A and 2B is presented in Fig. 3 *A*, which shows a scatterplot of the dil intensity vs the FITC-IgE intensity. Each point on the graph represents one pixel on the cell; the value of that pixel in the FITC-IgE image (Fig. 2 *A*) is the x-coordinate of the point, and the value of that pixel in the dil image (Fig. 2 *B*) is the y-coordinate. If the dil intensity were strictly proportional to the FITC-IgE intensity, the points on this plot would fall on a straight line. This is clearly not the case.

For the uncross-linked control cell of Fig. 1, *A* and *B*, the same scatterplot analysis is shown in Fig. 3 *B*. In this case, the intensities are confined to a narrow range of values, both for FITC-IgE and for dil. In contrast, Fig. 3 *A* shows that many pixels had higher intensities for both labels in the cross-linked cell image and a much wider distribution of observed intensities.

The formation of the large patches in Fig. 2 required warming the cells to 37°C for 10 min after they had been cross-linked for several hours at 4°C. In the absence of a warm-up period, numerous dispersed small patches of IgE are found over the cell surface. These small patches also show co-aggregation of dil (data not shown), but they are more difficult to analyze.

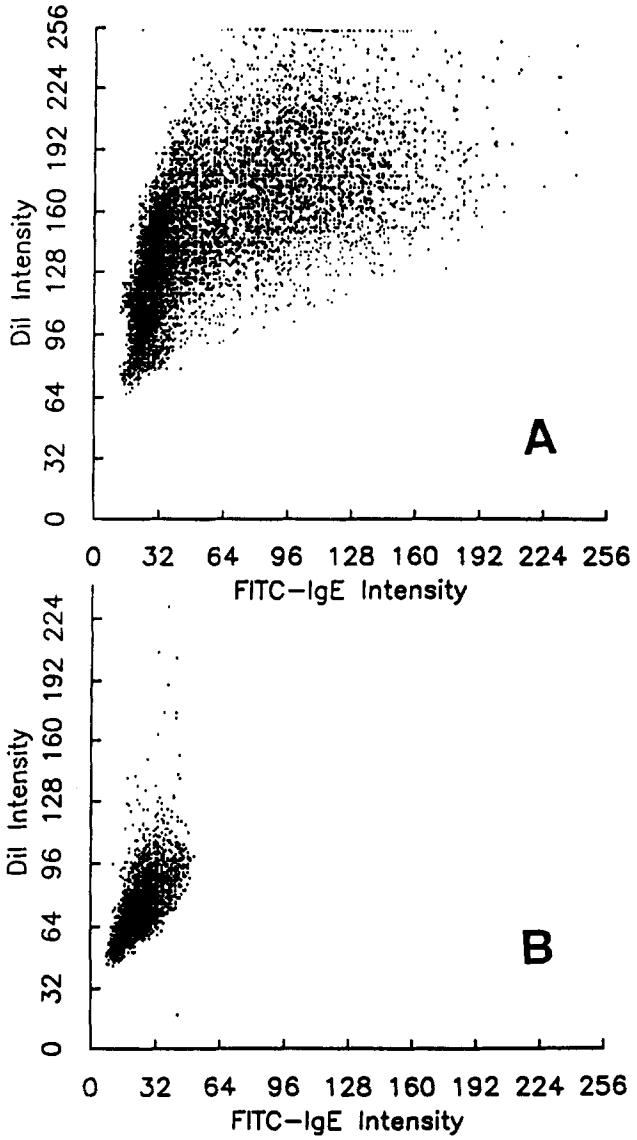

Figure 3. Scatterplots of dil intensity vs FITC-IgE intensity for the images of fluorescence distributions on the cross-linked cell in Fig. 2 *A* and *B* (*A*), and for the uncross-linked cell in Fig. 1, *A* and *B* (*B*).

DiI in Patches Is Largely Immobilized

To investigate the lateral mobility of the co-aggregated lipophilic probes, we carried out FPR experiments on patched and unpatched cells. A small spot (2.0 μm diam) was bleached in the dil fluorescence, and the recovery of fluorescence was monitored as described in Materials and Methods. On the cross-linked, patched cells, measurements of dil diffusion were made both on and off patches, as illustrated in Fig. 4. The top photograph in Fig. 4 shows an image of a patched cell in fluorescein optics. The center left photograph shows the same cell in dil optics, and the dotted circle on the patch near the center of the cell indicates where FPR was carried out. The fluorescence record is shown to the right; the entire time record is 50 s. During this time, very little recovery of the bleached fluorescence occurs, indicating that dye surrounding the bleached hole is unable to exchange freely with the bleached dye. The bottom left photograph of Fig. 4 shows the same cell, repositioned to bleach a non-patched region of the cell, following the FPR measure-

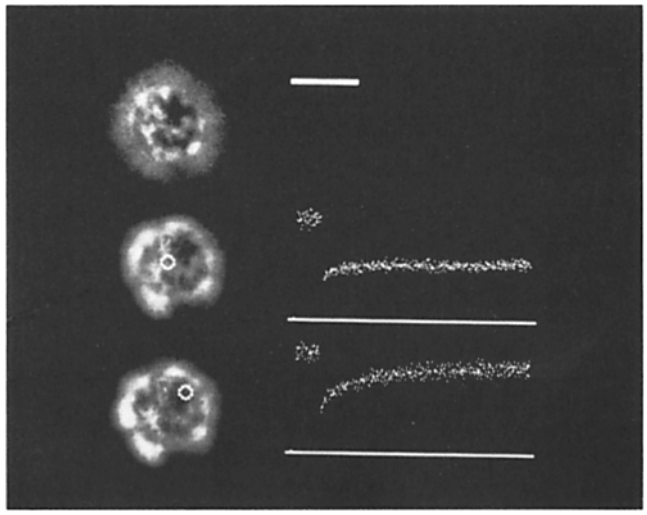

Figure 4. FPR measurements of dil mobility. (*Top*) RBL cell with FITC-IgE receptor complexes, focused near the top surface of the cell. The "halo" of fluorescence is due to out of focus regions on the sides of the cell. Bar, 10 μm. (*Center*) A bleaching experiment on a patched region of the same cell. An image of the cell in dil optics is shown at left. The dotted circle indicates the position and size of the bleaching spot. The fluorescence in the spot as a function of time is plotted on the right. The discontinuity in the fluorescence occurs due to the bleaching pulse. The time record displayed is 50 s. (*Bottom*) A bleaching experiment on a non-patched region of the same cell. An image of the cell in dil optics is shown at left. The dotted circle indicates the bleaching region, and the fluorescence time record is plotted at right, as above.

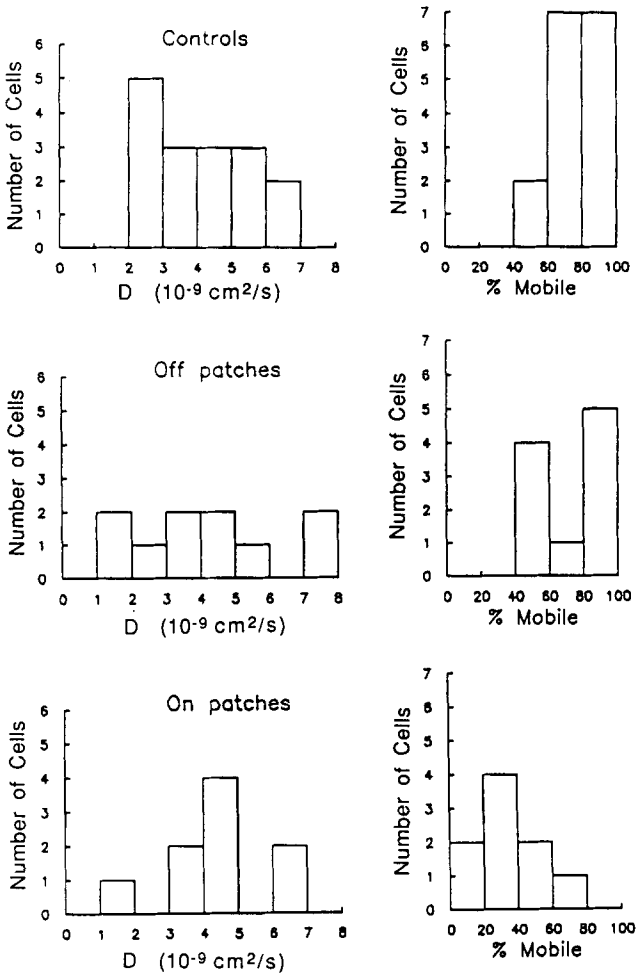

Figure 5. Summary of FPR results. Diffusion coefficients are shown at left, and mobile fractions at right. At the top, control uncross-linked cells, which have otherwise been treated in the same fashion as the patched cells. (*Center*) dil diffusion off of patches is similar to that from control cells. (*Bottom*) On patches, a smaller fraction of the dil is mobile (~35% compared with ~75% for *top* and *center*). The dil that is mobile in the patches has the same average diffusion coefficient as the dil outside of patches (~4 × 10^{-9} cm^2/s).

ment shown in the center panel. After this region was bleached, much more fluorescence recovery was obtained, as shown by the trace at the right. Note that the spot previously bleached in the patch appears darker than in the center, pre-bleach image, due to the lack of fluorescence recovery.

Quantitatively, FPR recovery curves were fit as described in Materials and Methods to obtain a diffusion coefficient and a mobile fraction. The results from all cells examined are presented in Fig. 5. Diffusion coefficients for dil on all cells have an average value of 4 × 10^{-9} cm^2/s, with no apparent difference between patched and unpatched regions of a cross-linked cell, or between uncross-linked and cross-linked cells. Mobile fractions, however, are significantly reduced in patches of dil: ca. 35% in patches vs ca. 75% in non-patched regions or on uncross-linked cells. In addition, the bleaching spot on a patch may contain some unpatched regions (some of which will be smaller than the microscope resolution limit), so that the mobile fraction measured on patches is an upper limit.

Co-aggregation Occurs with Some Other But Not All Lipophilic Probes

The co-aggregation of lipophilic probes with patches of IgE receptor does not appear to be specific to dil. Fig. 6 shows two cells that were labeled with ORB before cross-linking of the IgE receptors with anti-IgE for several hours at 4°C, followed by warming to 37°C for ten minutes to enhance aggregation. The right image is the distribution of ORB; the left image shows the patches of the IgE receptor. As with dil, most of the IgE receptor patches have coincident patches of ORB, although the intensity of the ORB patches is variable. ORB remains mostly at the plasma membrane under these conditions, as demonstrated by the lack of punctate label within the cell interior. On uncross-linked cells, ORB labels the plasma membrane uniformly (data not shown). In addition to ORB and dil, which are both positively charged, 5-(N-hexadecanoyl)aminoeosin, which is negatively charged, also appears to exhibit some colocalization with IgE receptor patches (data not shown).

Not all lipophilic probes co-aggregate, however. The probes tetramethylammonium diphenylhexatriene (23) and laurdan (22) both appear to have relatively uniform plasma membrane distributions when used to label RBL cells either with or without patched IgE receptors (data not shown).

Co-aggregation Is Not Specific to the IgE Receptor

DiI also co-aggregates when cell membrane constituents other than the IgE receptor are aggregated into large patches. Fig. 7 shows the distribution of dil (*right*) and the distribution of ganglioside aggregated via a specific monoclonal antibody, AA4, and a secondary antibody (*left*). There is clearly a strong correlation between the dil fluorescence and the ganglioside patches. Patching of a different cell surface antigen, recognized by the monoclonal antibody 3D12, also

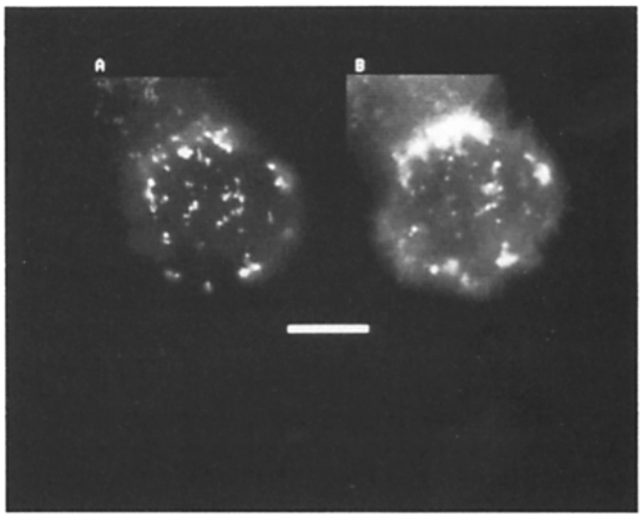

Figure 6. ORB colocalizes with IgE receptor patches on the surface of RBL cells. The left image (*A*) is the distribution of FITC-IgE, and the right image (*B*) is the distribution of ORB on the same cell. Bar, 10 μm.

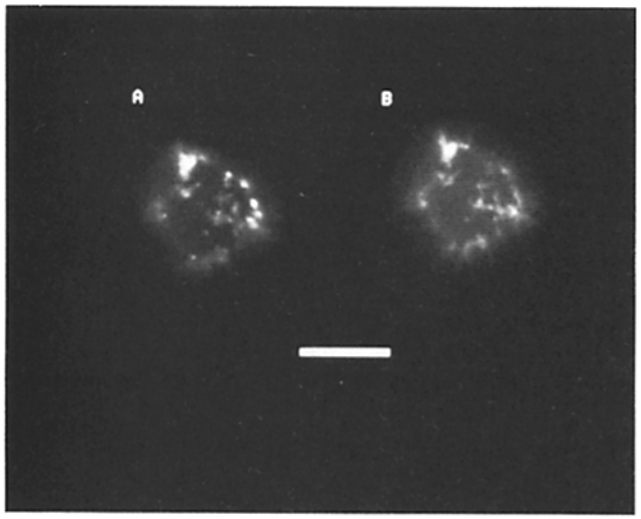

Figure 7. DiI colocalizes with a patched ganglioside at the cell surface. (Left) (*A*) Ganglioside patches formed with AA4 monoclonal anti-ganglioside antibody and an FITC-labeled polyclonal anti-IgG second antibody. (Right) (*B*) diI distribution in the same cell. Bar, 10 μm.

leads to co-aggregation of diI (data not shown). Neither of these surface antigens appears to be tightly associated with the IgE receptor, since immunoprecipitation of these solubilized antigens with their respective antibodies fails to bring down ^{125}I-IgE receptor complexes. Furthermore, cross-linking and internalization of the AA4 antibody bound to its antigen on the RBL cells does not cause aggregation and internalization of the IgE-receptor complexes (8).

Discussion

Our observations on the coredistribution of diI and other lipid probes with aggregated IgE receptors and other cell surface antigens provide new information on the structural organization of the plasma membrane of mammalian cells. Previous lateral diffusion studies using fluorescent lipid probes such as diI or NBD-C_6-PC, which label the plasma membrane and are slow to equilibrate with intracellular membranes, have generally indicated that these probes are not entirely free to diffuse as they would in homogeneous fluid phase liposomes. Both mobile fractions and diffusion coefficients are often observed to be somewhat smaller than expected for lateral diffusion in a simple fluid bilayer, but the structural basis for these observations is not well understood (15) (34). Our results indicate that the aggregation of a minor component of the plasma membrane, such as the IgE receptor, which makes up only about 1–2% of the cell surface proteins (25), causes the large-scale co-aggregation of a lipid analog which is present at a much higher density on the cell surface and which may reflect the coredistribution of endogenous lipid components as well. These results cannot be explained by observed morphological features of the plasma membrane, such as microvilli or ruffles in the region of receptor aggregates, since those features could not account for the loss of diI lateral mobility observed within the patches of receptor aggregates (34). Furthermore, Stump et al. (29) have shown that the regions of the cell surface containing large aggregates of IgE receptors are smooth and exclude the large ruffles which often surround them in activated RBL cells.

Co-aggregation Reflects a Change in Membrane Structure

Co-aggregation of lipid probes that accompanies the aggregation of membrane proteins must reflect a change in plasma membrane structure, and not simply an association of particular lipid analogs with the individual proteins being cross-linked. Several observations support this assertion:

(*a*) Co-aggregation of several different lipid analogs occurs with several different types of cross-linked membrane proteins. Both positively charged (diI and ORB) and negatively charged (5-(N-hexadecanoyl) aminoeosin) lipid analogs co-aggregated with the cross-linked IgE receptor. Most importantly, since each of three cell surface antigens separately caused co-aggregation of about half of the plasma membrane diI, much of the aggregated diI must have been either unassociated or reversibly associated with the antigens before cross-linking.

(*b*) The extent of co-aggregation does not appear to depend on the total amount of lipid probe that is associated with the plasma membrane, as qualitatively similar co-patching results are obtained over a wide range of diI concentrations in the membrane and in the labeling mixture (0.4–20 μM). Furthermore, even within a single field of cells, there is often a substantial cell to cell range of diI labeling intensities, yet all of the cells exhibit copatching of diI with FITC-IgE in which the fraction of diI co-aggregated is similar. For the standard labeling conditions, we estimate that there are between $\sim 10^7$ and 10^8 diI molecules per cell, and about half of these coredistribute with the IgE receptors, based on our quantitative analysis. Since there are $\sim 2 \times 10^5$ IgE receptors per RBL cell, this suggests a molar ratio of diI to IgE receptors in the patches of 50–500. This range is greater than the expected value of $\sim$12 phospholipids that could reasonably pack as nearest neighbors around a protein containing seven transmembrane-spanning segments, such as the IgE receptor (3). (This estimate for boundary lipid assumes a cylindrical protein with an intramembranous circumference that is similar to that for the 7-helix protein bacteriorhodopsin ($\leq$11 nm [11]) and the diameter of a phospholipid of $\sim$0.9 nm.) In this regard, it is interesting to note that the average density of IgE receptors in these patches is only about 1 per 350 nm^2, which is about five times more dense than unclustered receptors (Ryan, T. A., A. K. Menon, D. Holowka, B. Bard, and W. W. Webb. 1986. Inter-receptor spacing in IgE receptor aggregates on the surface of RBL cells. *Biophys. J.* 49:360a). Since each receptor probably has a cross-sectional area of $<$50 nm^2 in the membrane (as described above), the low receptor density in aggregates implies that other proteins and/or lipids must occupy most of the area within a patch of cross-linked receptors. Recent studies have indicated that most of the cellular proteins that are phosphorylated on tyrosine residues as the result of cross-linking receptors such as surface immunoglobulin on B cells are colocalized to patches of these receptors (30).

(*c*) Quantitative analysis of the CCD images of co-aggregated diI and FITC-IgE receptors indicates that there

is an approximate proportionality between the FITC intensity and the dil intensity as revealed by the scatterplots (Fig. 3). Fig. 3 *A* indicates that pixels with the highest intensities of FITC fluorescence tend to have a high intensity of dil fluorescence, but the dependence is quite variable, with a spread approaching a factor of two or three. The typical size of the coredistributed dil patches is somewhat greater than that of the FITC-IgE receptor patches, as is evident in Fig. 2, implying that the boundaries of the patches of dil do not exactly correspond to the boundaries of the patches of FITC-IgE receptors.

Possible Molecular Models for Coredistribution

In one model that is consistent with our observations, lipid probes that coredistribute with aggregated antigens are preenriched in optically undetectable fluid membrane domains which are "dragged along" into large patches by aggregation of the cell surface antigens. To account for the reduction of mobile fraction of dil that is observed in these aggregated domains, it is only required that these larger domains concentrate diffusional obstacles, or bind dil, to slow its escape from the patches. With the escape time $\tau_p \sim r_p^2/4D$, the increased patch radius r_p and/or decrease of D leads to slowed escape which is interpreted as increased immobile fraction in an FPR experiment. Increased binding energy would increase the dwell time of dil in the patches. The results of Edidin and Stroynowski (7) also indicate that dil in non-cross-linked cells is not confined to closed domains.

It is possible that the dil in the coredistributed patches becomes associated with some very abundant membrane protein or proteins that are themselves dragged into large patches by the cross-linking of less abundant cell surface proteins such as the IgE receptor. Preliminary results indicate that concanavalin A binding proteins do not coredistribute into patches of IgE receptors (Thomas, J., unpublished results), but it is possible that some other type of abundant protein, such as the agorins described by Apgar and Mescher (1) could be involved. It is possible that such interactions might be the consequence of changes in the membrane structure due to the activation of signal transduction processes (12). In this regard, it is notable that the conditions under which coredistribution of dil occurs also result in the loss of IgE receptor lateral mobility (20) and the loss of receptor solubilization by mild detergents (24). The detergent-insoluble, aggregated receptors appear to be stably associated with the cortical cytoskeleton (24). In the presence of mild detergents, coredistributed dil does not remain associated with the cytoskeleton-attached receptors, indicating that this association depends on the integrity of the membrane (Holowka, D., unpublished results). Preferential redistribution of certain membrane lipids due to this process could lead to the formation of gel-like membrane domains which are known to bind dil preferentially compared to more fluid membranes (36) (28). Alternatively, the formation of boundaries between fluid domains that do not allow the free exchange of dil molecules could also cause the observed loss of lateral mobility of coredistributed dil. The molecular nature of these hypothesized boundaries in this case is unknown, but recent results indicate that such boundaries can be created with certain cholesterol-binding agents such as filipin (9). Future experiments will distinguish between these different models.

In summary, the coaggregation of lipid analogs with cross-linked cell surface antigens demonstrates that cross-linking and patch formation do cause macroscopic (>1 μm) changes in the plasma membrane structure of RBL cells. The concentration of specific membrane proteins into patches alters the proximal plasma membrane in a fundamental way, trapping some lipid analogs in immobilized aggregates. These membrane changes might normally occur as a precursor to internalization, or as a facilitator of signal transduction or desensitization. At physiological temperatures, rapid internalization of small receptor aggregates normally prevents the observation of these unusual membrane domains. We have successfully used an extended incubation at 4°C to permit the formation of large protein aggregates, and we have observed significant concomitant changes in the plasma membrane organization.

This work was supported by National Institutes of Health (NIH) grants AI22449 and AI18306 (D. Holowka and B. Baird), National Science Foundation grant DIR 8800278, NIH grants T32 GM07273 and IRR04224A, and was based on the facilities of the NIH and National Science Foundation Developmental Resource for Biophysical Imaging and Optoelectronics (J. L. Thomas and W. W. Webb).

Received for publication 6 April 1993 and in revised form 16 November 1993.

References

1. Apgar, J. R., and M. F. Mescher. 1986. Agorins: major structural proteins of the plasma membrane skeleton of p815 tumor cells. *J. Cell Biol.* 103:351–360.
2. Basiano, L. K., E. H. Berenstein, L. Kirnak, and R. P. Siraganian. 1986. Monoclonal antibodies that inhibit IgE binding. *J. Biol. Chem.* 261: 11823–11839.
3. Blank, V., C. Ra, L. Miller, K. White, H. Metzger, and J.-P. Kinet. 1989. Complete structure and expression in transfected cells of high affinity IgE receptor. *Nature (Lond.).* 337:187–189.
4. Bloom, J., and W. Webb. 1983. Lipid diffusibility in the intact erythrocyte membrane. *Biophys. J.* 42:295–305.
5. Cowan, A., D. Myles, and D. Koppel. 1987. Lateral diffusion of the PH-20 protein on guinea pig sperm: evidence that barriers to diffusion maintain plasma membrane domains in mammalian sperm. *J. Cell Biol.* 104: 917–923.
6. Dictus, W., J. vanZoelen, P. Tetteroo, L. Tertoolen, S. deLaat, and J. Bluemink. 1984. Lateral mobility of plasma membrane lipids in Xenopus eggs: regional differences related to animal/vegetal polarity become extreme upon fertilization. *Dev. Biol.* 101:201–211.
7. Edidin, M., and I. Stroynowski. 1991. Differences between the lateral organization of conventional and inositol phospholipid-anchored membrane proteins. A further definition of micrometer scale membrane domains. *J. Cell Biol.* 112:1143–1150.
8. Estes, K. A. S. 1988. Studies of interactions between the receptor for immunoglobulin E and other cellular components during signal transduction. Ph.D., Cornell University, Ithaca, NY. 79–80.
9. Feder, T., E.-Y. Chang, D. Holowka, and W. Webb. 1994. Disparate modulation of plasma membrane protein lateral mobility by various permeabilizing agents. *J. Cell Physiol.* 158:7–16.
10. Guo, N., G. Her, V. Reinhold, M. Brennan, and R. Siraganian. 1989. Monoclonal antibody AA4 which inhibits binding of IgE to high affinity receptors on rat basophilic leukemia cells binds to novel alpha galactosyl derivatives of ganglioside G-D-1B. *J. Biol. Chem.* 264:13267–13272.
11. Henderson, R., and P. N. T. Unwin. 1975. Three-dimensional model of purple membrane obtained by electron microscopy. *Nature (Lond.).* 257:28–32.
12. Holowka, D., and B. Baird. 1992. Recent evidence for common signalling mechanisms among immunoreceptors that recognize foreign antigens. *Cell. Signalling.* 4:339–349.
13. Isersky, C., J. Rivera, S. Mims, and T. J. Triche. 1979. The fate of IgE bound to rat basophilic leukemia cells. *J. Immunol.* 122:1926–1936.
14. Jain, M., and H. White. 1977. Long range order in biomembranes. *Adv. Lipid Res.* 15:1–60.
15. Jovin, T. M., and W. L. C. Vaz. 1989. Rotational and translational diffusion in membranes measured by fluorescence and phosphorescence methods. *Meth. Enzymology.* 172:471–513.
16. Lemay, G., M. Zollinger, G. Waksman, B. Roques, and P. Crine. 1990. Recombinant neutral endopeptidase-24.11 expressed in mouse neuroblas-

toma cells is associated with neurite membranes. *Biochem. J.* 267: 447–452.
17. Lisanti, M., M. Sargiacomo, A. Saltiel, and E. Rodriguez-Boulan. 1988. Polarized apical distribution of glycosyl-phosphatidylinositol-anchored proteins in a renal epithelial cell line. *Proc. Natl. Acad. Sci. USA.* 85:9557–9561.
18. Maurice, M., E. Rogier, D. Cassio, and G. Feldman. 1988. Formation of plasma membrane domains in rat hepatocytes and hepatoma cell lines in culture. *J. Cell Sci.* 90:79–92.
19. Menon, A. K., D. Holowka, and B. Baird. 1984. Small oligomers of immunoglobulin E (IgE) cause large-scale clustering of IgE receptors on the surface of rat basophilic leukemia cells. *J. Cell Biol.* 98:577–583.
20. Menon, A. K., W. Webb, D. Holowka, and B. Baird. 1986. Crosslinking of receptor-bound IgE to aggregates larger than dimers leads to rapid immobilization. *J. Cell Biol.* 102:541–550.
21. Metzger, H. 1978. The IgE-mast cell system as a paradigm for the study of antibody mechanisms. *Immunological Rev.* 41:186–199.
22. Parasassi, T., F. Conti, and E. Gratton. 1990. Phase fluctuation in phospholipid membranes revealed by Laurdan fluorescence. *Biophys. J.* 5:1179–1186.
23. Prendergast, F. G., R. P. Haugland, and P. J. Callahan. 1981. 1-[4-(trimethylamino) phenyl]-6-phenylhexa-1,3,5-triene: synthesis, fluorescence properties, and use as a fluorescence probe of lipid bilayers. *Biochemistry.* 20:7333–7338.
24. Robertson, D., D. Holowka, and B. Baird. 1986. Cross-linking of immunoglobulin E-receptor complexes induces their interaction with the cytoskeleton of rat basophilic leukemia cells. *J. Immunol.* 136:4565–4572.
25. Ryan, T. A., J. Myers, D. Holowka, B. Baird, and W. Webb. 1988. Molecular crowding on the cell surface. *Science (Wash. DC).* 239:61–64.
26. Scher, M. G., and R. J. Bloch. 1991. The lipid bilayer of acetylcholine receptor clusters of cultured rat myotubes is organized into morphologically distinct domains. *Exp. Cell Res.* 195:79–91.
27. Singer, S., and G. Nicholson. 1972. The fluid mosaic model of the structure of cell membranes. *Science (Wash. DC).* 175:720–731.
28. Spink, C. H., M. D. Yeager, and G. W. Feigenson. 1990. Partitioning behavior of indocarbocyanine probes between coexisting gel and fluid phases in model membranes. *Biochim. Biophys. Acta.* 1023:25–33.
29. Stump, R. F., J. R. Pfeiffer, J. Seagrave, and J. M. Oliver. 1988. Mapping gold-labeled IgE receptors on mast cells by scanning electron microscopy: receptor distributions revealed by silver enhancement, backscattered electron imaging, and digital image analysis. *J. Histochem. Cytochem.* 36:493–502.
30. Takagi, S., M. Daibata, T. J. Last, R. E. Humphreys, D. C. Parker, and T. Sairenji. 1991. Intracellular localization of tyrosine kinase substrates beneath crosslinked surface immunoglobulins in B cells. *J. Exp. Med.* 174:381–388.
31. Thomas, J. L., and W. W. Webb. 1990. Fluorescence photobleaching recovery: a probe of membrane dynamics. *In* Noninvasive Techniques in Cell Biology. J. K. Foskett and S. Grinsteins, editors. Wiley-Liss, New York. 129–152.
32. Treistman, S., M. Moynihan, and D. Wolf. 1987. Influence of alcohols, temperature, and region on the mobility of lipids in neuronal membrane. *Biochem. Biophys. Acta.* 898:109–120.
33. Watson, L., Y.-H. Kang, and M. Falk. 1989. Cytochemical properties of osteoblast cell membrane domains. *J. Histochem. Cytochem.* 37:1235–1246.
34. Wolf, D. E. 1988. Probing the lateral organization and dynamics of membranes. *In* Spectroscopic Membrane Probes. L. M. Loew, L. M. Loews, editors. CRC Press, Boca Raton, FL. 193–220.
35. Wolf, D., M. Edidin, and A. Handyside. 1981. Changes in the organization of the mouse egg plasma membrane upon fertilization and first cleavage: indications from the lateral diffusion rates of fluorescent lipid analogs. *Dev. Biol.* 85:195–198.
36. Wolf, D., W. Kinsey, W. Lennarz, and M. Edidin. 1981. Changes in the organization of the sea urchin egg plasma membrane upon fertilization: indications from the lateral diffusion rates of lipid-soluble fluorescent dyes. *Dev. Biol.* 81:133–138.
37. Yechiel, E., and M. Edidin. 1987. Micrometer-scale domains in fibroblast plasma membranes. *J. Cell Biol.* 105:755–760.
38. Yechiel, E., Y. Barenholz, and Y. Henis. 1985. Lateral mobility and organization of phospholipids and proteins in rat myocyte membranes. *J. Biol. Chem.* 260:9132–9136.
39. Yguerabide, J., J. Schmidt, and E. Yguerabide. 1982. Lateral mobility in membranes as detected by fluorescence recovery after photobleaching. *Biophys. J.* 39:69–75.